Cancer Letters 521 (2021) 71–81

Contents lists available at ScienceDirect

Cancer Letters

journal homepage: www.elsevier.com/locate/canlet

ZIP4 promotes non-small cell lung cancer metastasis by activating snail-N-cadherin signaling axis

Yuanyuan Jiang [a,b,c], Hanxiang Zhan [b,c,d], Yuqing Zhang [b,c], Jingxuan Yang [b,c], Mingyang Liu [b,c], Chao Xu [e], Xiao Fan [f], Junxia Zhang [b,c,f], Zhijun Zhou [b,c], Xiuhui Shi [b,c], Rajagopal Ramesh [g], Min Li [b,c,*]

[a] Department of Pulmonary and Critical Care Medicine, Qilu Hospital, Shandong University, Jinan, Shandong, China
[b] Department of Medicine, the University of Oklahoma Health Sciences Center, Oklahoma City, OK, USA
[c] Department of Surgery, the University of Oklahoma Health Sciences Center, Oklahoma City, OK, USA
[d] Department of General Surgery, Qilu Hospital, Shandong University, Jinan, Shandong, China
[e] Department of Biostatistics and Epidemiology, Hudson College of Public Health, the University of Oklahoma Health Sciences Center, Oklahoma City, OK, USA
[f] Department of Neurosurgery, the First Affiliated Hospital of Nanjing Medical University, Nanjing, Jiangsu, China
[g] Department of Pathology, the University of Oklahoma Health Sciences Center, Oklahoma City, OK, USA

ARTICLE INFO

Keywords:
ZIP4
Non-small cell lung cancer
Snail
Epithelial-mesenchymal transition
Metastasis

ABSTRACT

Non-small cell lung cancer (NSCLC) is one of the most critical health problems worldwide, with high incidence and poor survival rate. A zinc importer ZIP4 has been implicated in the process of tumor growth and metastasis of many cancers. However, its exact role and the underlying mechanism in NSCLC remains to be elucidated. In the present study, we found that human ZIP4 was substantially overexpressed in NSCLC tissues and was correlated with poor overall survival (OS) and progression-free survival (PFS). Overexpression of ZIP4 promoted cell migration, invasion and metastasis both *in vitro* and in a mouse lung metastasis model. Silencing of ZIP4 attenuated migration, invasion and metastasis. Mechanistically, overexpression of ZIP4 increased the expression of Snail, Slug and N-cadherin while genetic inactivation of ZIP4 downregulated the expression of above-mentioned genes. Further analysis showed that transcriptional factor Snail which modulates N-cadherin was involved in the process of ZIP4-mediated NSCLC migration and invasion. We also demonstrated that ZIP4 positively correlates with the levels of Snail, Slug and N-cadherin in mice lung metastasis tumors. Together, these results suggest that ZIP4 acts as an important regulator of Snail-N-cadherin signaling axis in promoting NSCLC progression and may serve as a novel predictive marker and therapeutic target in NSCLC.

1. Introduction

Lung cancer is the leading cause of death from all cancer types worldwide (18.4% of all cancer deaths) [1]. It can be divided into small cell lung cancer (SCLC) and non-small cell lung cancer (NSCLC). NSCLC is the most common subtype whose five-year survival rate is only 15%, with approximately 70% of NSCLC patients diagnosed with metastases [2]. Histologically NSCLC has different subtypes exhibiting distinct disease patterns and cellular heterogeneity [3,4]. Even though great progress has been made in the diagnosis and treatment of NSCLC, the morbidity and mortality still remain high. And little is known about the pathogenesis and molecular mechanism of NSCLC [4,5]. Therefore, there is a pressing need to identify new markers and therapeutic targets to develop an effective treatment for NSCLC.

Zinc is an essential trace element and nutrient functioning as a catalytic cofactor for multiple enzymes; and it is required for many enzymes and transcriptional regulators involved in cancer growth and metastasis [6]. Zinc concentrations are maintained by two zinc carrier families: intracellular zinc concentration is increased by ZIP family through promoting extracellular uptake, while reduced by ZnT transporters through efflux [6–8]. Aberrant expression of ZIP family leading to altered intracellular zinc levels are involved in the pathogenesis of multiple cancers such as pancreatic cancer [6,9,10], glioblastoma [11,12], breast cancer [13], and prostate cancer [14]. ZIP4 is overexpressed

* Corresponding author. Department of Medicine, Department of Surgery The University of Oklahoma Health Sciences Center 975 NE 10th Street, BRC 1262A, Oklahoma City, OK, 73104, USA.
E-mail address: Min-Li@ouhsc.edu (M. Li).

https://doi.org/10.1016/j.canlet.2021.08.025
Received 12 July 2021; Received in revised form 16 August 2021; Accepted 22 August 2021
Available online 24 August 2021

in human pancreatic cancer and promoted tumor growth and progression [9]. ZIP4-ZEB1-Integrin α3β1 pathway mediated gemcitabine resistance of pancreatic tumors by inhibiting ENT1 expression [15]. Our previous study described a complete gene expression profiling of zinc transporters (14 ZIPs and 10 ZnTs proteins) in human lung cancer tissues and cell lines and found there were differential expression patterns of zinc transporters which showed high tissue specificity [16]. However, the molecular mechanisms underlying the zinc transporter mediated NSCLC metastasis require further investigation.

In this study, we found that ZIP4 was overexpressed in NSCLC tumor tissue, and its expression level negatively correlated with overall survival (OS) and progression-free survival (PFS) in patients with NSCLC. Both *in vitro* and *in vivo* studies revealed that ZIP4 can promote NSCLC tumor invasion, migration and metastasis. Mechanistically, ZIP4 can facilitate epithelial-mesenchymal transition (EMT) process and increase NSCLC cancer cell metastasis via activating Snail-N-cadherin signaling pathway. In summary, our study uncovers a novel mechanism of the progression and metastasis of NSCLC mediated by the ZIP4-Snail-N-cadherin axis, and also suggests that ZIP4 may serve as a novel prognostic biomarker and a potential therapeutic target for NSCLC.

2. Materials and methods

2.1. Tissue microarray (TMA) based immunohistochemical (IHC) staining

A TMA containing 98 pairs of lung adenocarcinoma and adjacent tissue samples (2 mm tissue core per replicate) and another TMA containing 90 pairs of lung squamous carcinoma and adjacent tissue samples were constructed by Outdo Biotech Co., Ltd. (Shanghai, China). And the clinicopathological and survival data were also provided by Outdo Biotech Co., Ltd. None of the patients received neoadjuvant chemotherapy or radiotherapy prior to surgery, and all patients have completed 5 years follow-up process. A rabbit polyclonal antibody against human ZIP4 (Proteintech, dilution: 1:100) and a two-step immunohistochemical staining kit (EnVisionTM + kit, Dako, Denmark) were used. The staining intensity and the proportion of immunostained tumor were assessed and the staining intensity was defined as the follows: 0, negative; 1, weak; 2, moderate; or 3, strong according to a previous study [17]. The staining index was obtained by these two scores multiplied. A high ZIP4 expression was defined as a staining index >1.8, whereas a low ZIP4 expression ≤ 1.8.

2.2. Database analysis

Gene expression profiling data of NSCLC patients was obtained from the GEO Datasets (GSE30219 GSE10072) (https://www.ncbi.nlm.nih.gov/geo/). For the survival analysis, we included multiple data sets, including TCGA, CAARRAY, GSE14814, GSE19188, GSE29013, GSE30219, GSE10072, GSE31210, GSE3141, GSE31908, GSE37745, GSE43580, GSE4573, GSE50081 and GSE8894, which were incorporated in the Kaplan-Meier Plotter platform (https://kmplot.com/analysis/). Median value of ZIP4 expression was set as the cut-off value. To elucidate the function of ZIP4 in NSCLC, we screened gene ontology term differences by DAVID analysis using positively associated genes of ZIP4 ($R > 0.3$). Data were obtained from the public databases and all the patients' information were de-identified, ethical approval was waived by institutional ethics committee.

2.3. Cell culture

A549 and H358 lung cancer cell lines were kindly provided by Dr. Rajagopal Ramesh from the University of Oklahoma Health Sciences Center (OUHSC). All the cells were cultured in RPMI-1640 medium (HyClone) containing with 10%FBS (fetal bovine serum) (Gibco by life technologies), 1% penicillin/streptomycin (Sigma) and 1% Sodium Pyruvate (Gibco) at 37 °C with 5% CO_2.

2.4. Stable cell line construction

Our previous study detected the expression level of ZIP4 in 8 different lung cancer cell lines, and found low expression of ZIP4 in A549 cell and high expression in H358 cell line [16], so we chose these two cell lines in the present study. ZIP4 overexpression cells were selected in A549 cells with retrovirus vector pBabe (Clontech), following manufacturer's instructions. Briefly, full-length human ZIP4 cDNA was cloned into pBabe vector, and the recombinant plasmid was transfected into phoenix ampho cells to prepare the viral particles used for A549 stable cell line selection. ZIP4 knockdown cells were selected in H358 cells with ZIP4 shRNA vector as described previously [6]. Recombinant plasmid was transfected into 293Ta cells together with packaging vectors. The viral supernatants were collected and transduced into A549 and H358 cells. Stable cells A549-V, A549-ZIP4 and H358-shV, H358-shZIP4 were selected with 0.5 μg/ml puromycin. The cells used in mouse lung metastasis model were transduced with viral vector expressing luciferase and GFP, so that the pulmonary metastatic nodules can be counted with a luminometer and under a UV filter. ZIP4 knockout cells were selected in H358 cells. Briefly, H358 cells were transfected with Cas9 expression vector (Addgene, MA) and selected with 2.5 μg/ml blasticidin, and then guide RNAs (gRNA) targeting ZIP4 were introduced into the H358-Cas9 cells by transfection using lipofectamine 3000. Finally, the monoclonal H358-ZIP4-knockout cells were selected by limiting dilution method.

2.5. RNA extraction and real-time PCR

ZIP4, Snail, Slug, N-cadherin, E-cadherin and Vimentin mRNAs expression levels were analyzed by real-time PCR using the SYBR supermix kit (Life Technologies). Briefly, the PCR reaction which including 100 nmol/L primer, diluted cDNA templates, and SYBR Green supermix running for 40 cycles at 95 °C for 20 s and then 60 °C for 1 min. Each cDNA sample was run in triplicate andβ-actin primer was included in every plate in order to avoid sample variations. The primer sequences are as follows:

Gene		Sequence (5′-3′)
ZIP4	F	ATGTCAGGAGCGGGTCTTGC
	R	GCTGCTGTGCTGCTGGAAC
Snail	F	TCGGAAGCCTAACTACAGCGA
	R	AGATGAGCATTGGCAGCGAG
Slug	F	CGAACTGGACACACATACAGTG
	R	CTGAGGATCTCTGGTTGTGGT
N-cadherin	F	TTTGATGGAGGTCTCCTAACACC
	R	ACGTTTAACACGTTGGAAATGTG
E-cadherin	F	CGAGAGCTACACGTTCACGG
	R	GGGTGTCGAGGGAAAAATAGG
Vimentin	F	AGTCCACTGAGTACCGGAGAC
	R	CATTTCACGCATCTGGCGTTC

2.6. Western Blot analysis

Cell lysates were collected and loaded on 8% SDS polyacrylamide gels then transferred to a nitrocellulose membrane (Life Technologies). The membranes were incubated with antibodies against ZIP4 (Proteintech, 1:2000), Snail (Cell signaling, 1:1000), Slug (Cell signaling, 1:1000), N-cadherin (Cell signaling, 1:1000), E-cadherin (Cell signaling, 1:1000), Vimentin (Cell signaling, 1:1000) or β-actin (Sigma, 1:10000) at 4 °C overnight. Following washes with TBST, membranes were incubated with the secondary antibody diluted into milk (1: 20,000) for 1 h at room temperature. After washing by TBST for 3 times, the membranes were detected using an enhanced chemiluminescent (ECL) plus reagent kit.

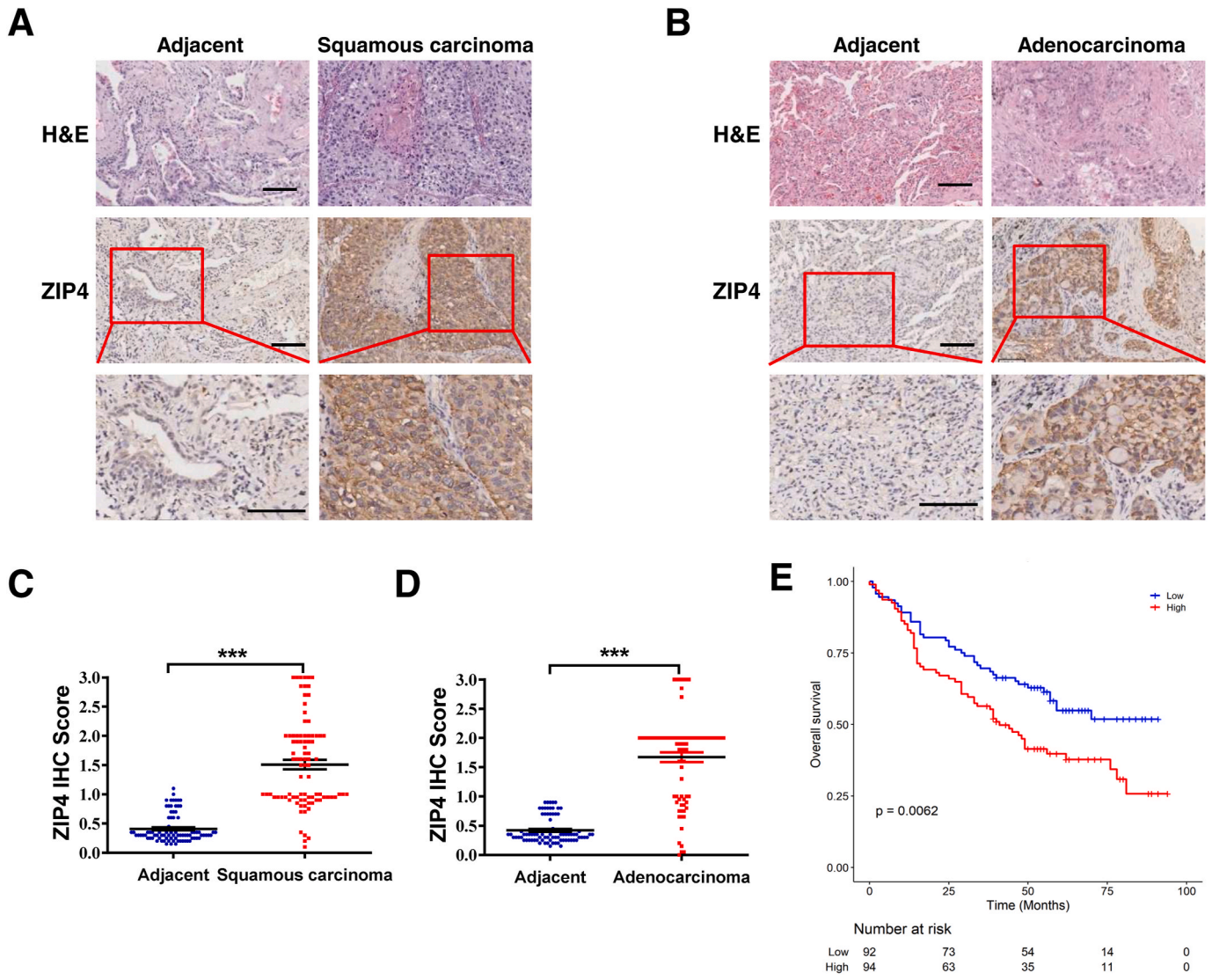

Fig. 1. ZIP4 is overexpressed in non-small cell lung cancer and is negatively correlated with patients' overall survival (OS). **(A)** Representative images of H&E and IHC staining of ZIP4 in human lung squamous carcinoma and adjacent tissues. Scale bar, 100 μm. **(B)** Representative images of H&E and IHC staining of ZIP4 in human lung adenocarcinoma and adjacent tissues. Scale bar, 100 μm. **(C)** IHC score of ZIP4 staining in human lung squamous carcinoma and adjacent tissues. $^{***}P < 0.0001$ vs. adjacent tissues, using paired *t*-test. **(D)** IHC score of ZIP4 staining in human lung adenocarcinoma and adjacent tissues. $^{***}P < 0.0001$, using paired *t*-test. **(E)** The association between ZIP4 expression and patients' overall survival (OS) in human lung NSCLC patients. $P = 0.0063$. The cut-off value of ZIP4 IHC score is 1.8.

2.7. In vitro wound healing assay

Cells were seeded in 6-well plates and treated with mitomycin C (10 μg/ml, Sigma) for 2 h after they grew to about 90%–100% confluent. 100 μl pipette tips were used to make the scraped lines and the wound healing was detected and images were recorded at 0 and 48 h under a microscope. The images acquired for each sample were further analyzed quantitatively. For each image, distances between one side of scratch and the other were measured at certain intervals (μm) using Image Pro-Plus software (Media Cybernetics) and calculated as percentage of migration distance normalized to the scratch distance at 0 h.

2.8. In vitro migration and invasion assay

Modified Boyden chamber with uncoated or coated matrigel were used to detect the cell migration or invasion (Corning). Cells were trypsinized and resuspended in medium without FBS (5×10^4 cells/100 μl for migration and 5×10^4 cells/500 μl for invasion) and seeded into the upper chamber, with 600 μl of the growth medium added to the lower chamber (750 μl in lower chamber for invasion assay). 48 h later, cells were fixed with 20% methanol and stained with Crystal Violet for imaging and cell counting.

2.9. In vitro cell proliferation assay

Cell proliferation was tested by MTT assay. Stable cell lines A549-V, A549-ZIP4, H358-shV, H358-shZIP4 were seeded in 96-well plates (2000 cells/well), and serum-starved for 24 h. Cell growth was assessed on 0, 1, 2, 3, 4, 5 days. 20 μl per well of 50 mg/ml 3-(4, 5-dimethylthiazolyl-2)-2,5-diphenyltetrazolium bromide (MTT) solution (Applichem, Darmstadt, Germany) was added to cells. Cells were incubated for 4 h until a purple precipitate was visible. Precipitates were dissolved with DMSO by gentle shaking. And absorbance was measured at 490 nm with an EL-800 universal microplate reader (Bio-Tek Instruments, Winooski, VT).

2.10. In vivo subcutaneous (SC) tumor growth assay

Stable lung cancer cell lines (A549-V, A549-ZIP4, H358-shV, H358-shZIP4) were harvested by trypsinization and resuspended in RPMI-1640 medium. 5×10^6 A549 cells and 7.5×10^6 H358 cells in 100 μl medium were subcutaneously injected into the right flank of 6-week-old nude mice. Tumor growth was examined every week by a digital caliper, and the tumor volume was determined with the formula: tumor volume [mm^3] = (length [mm]) × (width [mm])^2 × 0.52. Five weeks later, all mice were euthanized by an overdose of CO_2 exposure and tumor weight was measured.

2.11. In vivo metastasis mouse model

The metastasis lung cancer mouse model was established by using tail vein injection of NSCLC cells as previously described [18,19]. In our study, stable lung cancer cell lines (A549-V, A549-ZIP4, H358-shV, H358-shZIP4) labelled with GFP and luciferase were used to establish lung metastasis mouse model in order to investigate the effect of ZIP4 on cell migration and invasion *in vivo*. Cells were harvested by trypsinization and then resuspended in RPMI-1640 medium. 2×10^6 A549 cells and 7×10^5 H358 cells in 100 μl medium were injected into the tail vein of 6-week-old nude mice with eleven nude mice in A549 groups and five nude mice in H358 groups (Envigo, Indianapolis). Luminescence in lung tumors was monitored with *in vivo* imaging system (IVIS) at 1, 2, 3 weeks after tail vein injection. Mice were intraperitoneal injected with 150 mg/kg luciferin (Gold Biotechnology) 20 min before imaging. Tumor burden was determined by averaging photon flux of mice. Three weeks after tail vein injection, all mice were euthanized and perfused using formalin. The pulmonary metastatic nodules with GFP signals were counted with a filter under UV. The lungs were fixed in formalin, paraffin-embedded sections of each lung tissue were stained with H&E and immunohistochemistry staining. All studies were approved by Institutional Animal Care and Use Committee (IACUC) at OUHSC.

2.12. IHC staining

Mouse lung paraffin embedded tissues were collected and prepared into 5-μm slides. Fixed tissue slides were incubated in 3% H_2O_2/methanol to quench endogenous peroxidase activity for 15 min and then washed with PBS. The slides were transferred into the container with antigen unmasking solution in the steamer and cooked for 20 min and then incubated in blocking buffer for 30 min at room temperature. Slides were stained with antibodies against ZIP4 (Proteintech, 1:500), Snail (Cell signaling, 1:200), Slug (Novus, 1:250), N-cadherin (Cell signaling, 1:200) and incubated overnight at 4 °C. After washing with PBS for 3 times, the slides were incubated with secondary antibody for 30 min at room temperature. Immune complexes were detected with diaminobenzidine (DAB) under a phase-contrast microscope. The staining intensity and the proportion of immunostained tumor were assessed. Positive control and controls without primary antibody were also included in all our experiments to make sure the staining quality. The slides were observed under a phase-contrast microscope and the staining intensity and proportion of immunostained tumor was scored by two pathologists without knowledge of the mice information.

2.13. Statistical analysis

Statistics analysis was performed in R (https://www.bioconductor.org/) and Graphpad Prism 6.0 software (https://www.graphpad.com). All values are expressed as mean ± standard deviation (SD). The statistical significance between experimental group and control was determined by Student's t-test or Wilcoxon's test. Chi-square, McNemar test or Kaplan–Meier analysis and Cox Proportional Hazard model were employed to assess the survival rate of patients. *P-value* less than 0.05 was considered to be a statistically significant difference.

Table 1
Differential expression of ZIP4 in NSCLC and adjacent tissues.

	n	ZIP4 expression		Chi-square Value	*P* value
		High	Low		
Adenocarcinoma	81	49	32	70.248	<0.0001
adjacent tissues	81	0	81		
Squamous carcinoma	88	32	56	39.111	<0.0001
adjacent tissues	88	0	88		

Table 2
Correlation between ZIP4 expression and clinicopathological characteristics in NSCLC.

	High variables	ZIP4 expression		Low total	χ2	*P* value
		low	high			
Age (year)					0.093	0.76
	≤58	36	33	69		
	>58	58	59	117		
Sex					0.845	0.358
	Female	21	27	48		
	male	71	67	138		
TNM stage					4.946	0.026
	I/II	67	55	122		
	III/IV	22	37	59		
T stage					0.268	0.605
	T1/T2	65	68	133		
	T3/T4	24	21	45		
N stage					1.199	0.655
	N0	47	45	92		
	N1/N2/N3	43	47	90		
M stage					1.979	0.16
	M0	92	92	184		
	M1	0	2	2		
Grade					7.411	0.006
	I/II	71	55	126		
	III	21	39	60		

3. Results

3.1. ZIP4 is overexpressed in NSCLC and its expression predicts patient survival

We examined the expression levels of ZIP4 in NSCLC tumor and adjacent tissues with TMA array by IHC staining. As shown in Fig. 1A and B, ZIP4 was predominantly expressed in the cytoplasm and cytomembrane in both lung squamous and adenocarcinoma cancer. High expression of ZIP4 was detected in 36.4% (32/88) of squamous carcinoma and 60.5% (49/81) of lung adenocarcinoma cancer tissues, respectively, while none of the adjacent tissues showed high ZIP4 expression ($P < 0.0001$, Table 1, Fig. 1C and 1D). We also investigated the correlation between ZIP4 expression and clinicopathological characteristics both in squamous carcinoma and adenocarcinoma patients. As shown in Table 2, high ZIP4 expression was associated with advanced stage and higher grade in NSCLC. The value of ZIP4 in predicting prognosis in patients with NSCLC was evaluated by univariate and multivariate Cox regression analysis. Univariate analysis revealed that patients with high ZIP4 expression, high tumor grade and advanced TNM stage had significantly worse overall survival ($P = 0.007$, 0.005 and $P < 0.0001$, respectively, Table 3). Multivariate Cox regression analysis identified ZIP4 expression (HR = 1.591, $P = 0.033$), tumor grade (HR = 1.631, $P = 0.027$) and TNM stage (HR = 2.687, $P = 0.002$) as independent prognostic factors in patients with NSCLC (Table 3). Kaplan–Meier survival analysis revealed that NSCLC patients with high expression of ZIP4 had much worse survival than those patients with low expression ($P = 0.0062$) (Fig. 1E). Meanwhile, in order to validate our finding, we also examined other data sets. We included multiple data

Table 3
Univariate and multivariate analyses of the factors correlated with overall survival of NSCLC patients.

variables	Univariate analysis			Multivariate analysis		
	HR	95%CI	p value	HR	95%CI	*P* value
ZIP4 expression	1.737	1.161–2.598	0.007	1.591	1.016–2.438	0.033
Age	1.555	1.01–2.393	0.045	1.45	0.911–2.306	0.117
sex	0.823	0.53–1.276	0.383	0.795	0.161–3.941	0.779
TNM stage	4.025	2.666–6.075	<0.0001	2.687	1.445–4.995	0.002
T stage	1.857	1.201–2.872	0.005	1.206	0.727–2.000	0.469
N stage	2.576	1.697–3.91	<0.0001	1.396	0.780–2.499	0.261
M stage	2.419	0.595–9.839	0.217	2.158	0.238–19.550	0.494
Grade	1.785	1.191–2.674	0.005	1.631	1.057–2.517	0.027

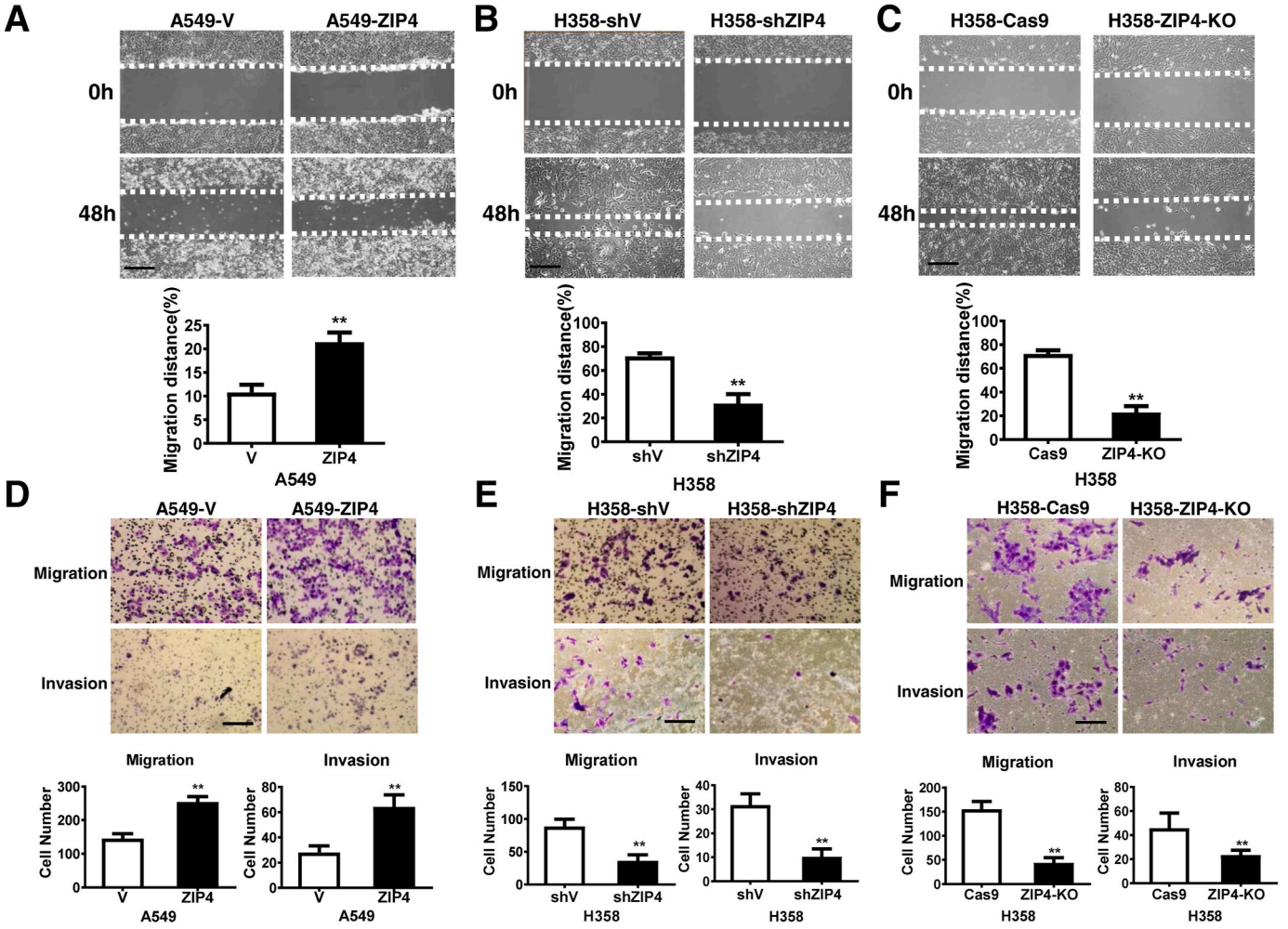

Fig. 2. ZIP4 promotes migration and invasion of NSCLC *in vitro*. **(A)** Wound healing assay. The view of wound healing was captured at 0 and 48 h in A549-V and A549-ZIP4 cells. ($P < 0.01$, *t*-test, n = 10). The migration distance was quantified and plotted. **(B)** Wound healing assay. The view of wound healing was captured at 0 and 48 h in H358-shV and H358-shZIP4 cells. ($P < 0.01$, *t*-test, n = 10). The migration distance was quantified and plotted. **(C)** Wound healing assay. The view of wound healing was captured at 0 and 48 h in H358-Cas9 and H358-ZIP4-KO cells. ($P < 0.01$, *t*-test, n = 10). The migration distance was quantified and plotted. **(D)** Transwell migration and invasion assay. Relative cell migration and invasion capacity was detected in A549-V and A549-ZIP4 cells at 48 h. ($P < 0.01$, *t*-test, n = 10). **(E)** Transwell migration and invasion assay. Relative cell migration and invasion was detected in H358-shV and H358-shZIP4 cells at 48 h. ($P < 0.01$, *t*-test, n = 10). **(F)** Transwell migration and invasion assay. Relative cell migration and invasion was detected in H358-Cas9 and H358-ZIP4-KO cells at 48 h. ($P < 0.01$, *t*-test, n = 10). All data are mean ± SD. Scale bar, 100 μm. **, $P < 0.01$.

sets which were incorporated in the Kaplan-Meier Plotter platform (https://kmplot.com/analysis/). We found that high ZIP4 expression in tumor tissue was associated with worse overall survival in NSCLC (Fig. S1A). In addition, we also assessed the association between ZIP4 expression levels and NSCLC patients' overall survival and progression-free survival with the data of GSE30219. The NSCLC patient overall survival and progression-free survival were significantly reduced in the group with high ZIP4 expression (Fig. S1B). To identify the function of ZIP4 involved in NSCLC, we screened gene ontology term differences by DAVID analysis using positively associated genes of ZIP4 (R > 0.3). Gene ontology term data showed that ZIP4 was associated with cell-cell adhesion, which was EMT related phenotype, in cell component (CC), molecular function (MF) and biological process (BP) (Fig. S1C). Further, gene set enrichment analysis (GSEA) revealing that ZIP4 was highly

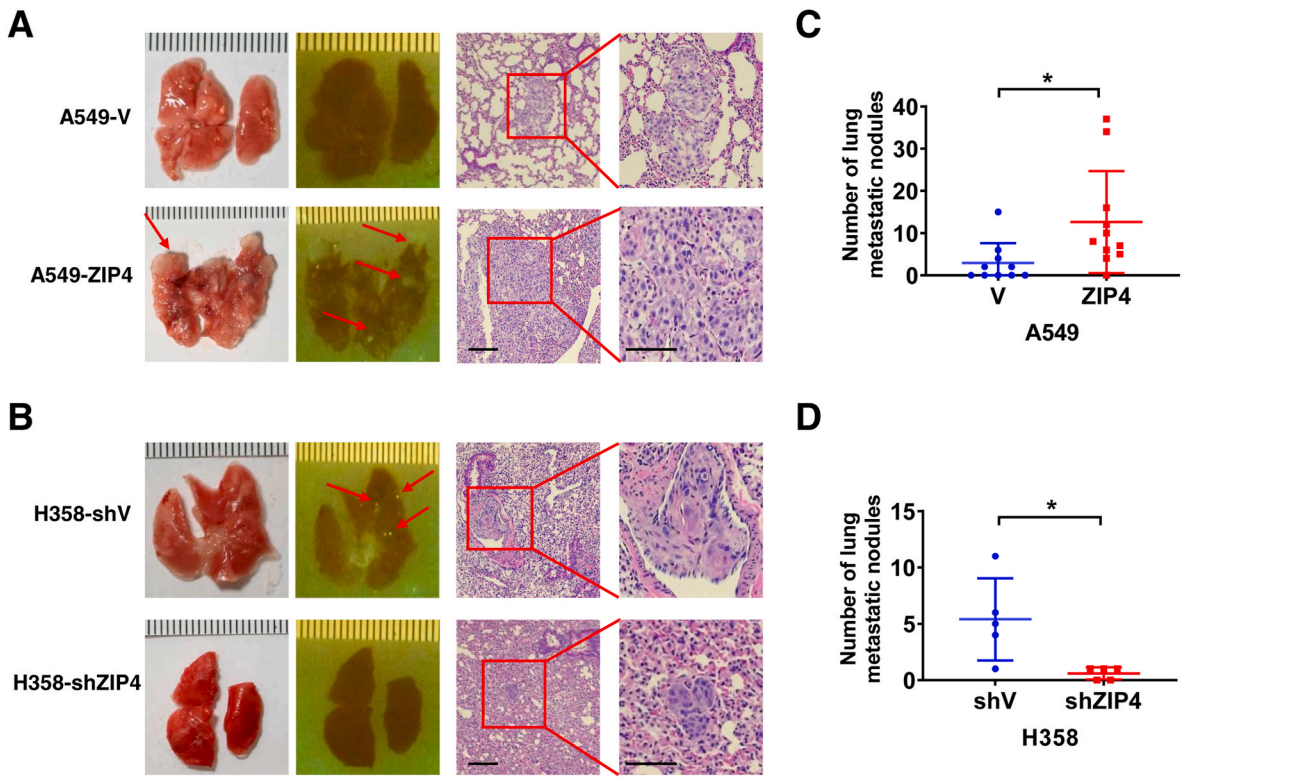

Fig. 3. ZIP4 promotes NSCLC metastasis *in vivo*. **(A)** Representative images of mouse lungs, GFP-expressing lung metastatic nodules under a UV filter and the H&E staining of lung tissues in A549-V and A549-ZIP4 xenograft mouse groups (the arrows refer to tumor lesions). **(B)** Representative images of mouse lungs, GFP-expressing lung metastatic nodules under a UV filter and the H&E staining of lung tissues in H358-shV and H358-shZIP4 xenograft mouse groups (the arrows refer to tumor lesions). **(C)** Plot of the numbers of lung metastatic nodules in A549-V and A549-ZIP4 xenograft mouse groups. **(D)** Plot of the numbers of lung metastatic nodules in H358-shV and H358-shZIP4 xenograft mouse groups. Scale bar, 100 μm. *$P < 0.05$.

involved in epithelial mesenchymal transition both in GSE30219 and GSE10072 datasets (Figs. S1D–S1E).

3.2. ZIP4 promotes NSCLC cell migration and invasion

Since ZIP4 has been indicated to play important roles in EMT and metastasis, we sought to investigate the ZIP4 function in cell migration and invasion in NSCLC. Firstly, the overexpression and blocking efficiency in the ZIP4 overexpression and knockdown stable cell lines were confirmed at mRNA and protein levels by RT-PCR and Western Blot analysis (Figs. S2A–S2C). The effect of ZIP4 on cell migration was examined by wound healing assay. A549-ZIP4 cells showed significantly faster closure of the wound area than A549-V cells (Fig. 2A; $P < 0.01$). Conversely, the migratory capability of H358-shZIP4 cells and H358-ZIP4-KO cells were dramatically reduced compared with the vector control cells (Fig. 2B and 2C; $P < 0.01$). In accordance with the wound healing assay results, transwell assays also showed that NSCLC cell migration and invasion were increased in ZIP4 overexpressed cells (Fig. 2D) and reduced in ZIP4 knockdown (Fig. 2E) and knockout cells (Fig. 2F) compared with the control cells. However, MTT results showed that ZIP4 overexpression or knockdown did not affect the cell proliferation rates of A549 and H358 cells (Figs. S3A–S3B). Thus, these results indicated that ZIP4 promotes the migration and invasion of NSCLC cells.

3.3. ZIP4 promotes NSCLC metastasis in vivo

To evaluate the functional impact of ZIP4 on tumor metastasis, A549-V, A549-ZIP4, H358-shV, H358-shZIP4 cells labelled with GFP and luciferase were injected into nude mice via tail vein. The images in Fig. S4A showed there were no difference of GFP signal between the paired stable cell lines of A549-V and A549-ZIP4, as well as in H358-shV and H358-shZIP4 cells. The signal of NSCLC cell metastasis to lung was monitored by luminescence using *in vivo* imaging system (IVIS), the results showed that the luminescent signals were stronger in A549-ZIP4 mice than that in A549-V mice and weaker in H358-shZIP4 mice than H358-ShV mice at 2 weeks and 3 weeks after tail vein injection (Fig. S4B). After 3 weeks of tumor growth and metastasis, mice in A549-ZIP4 group exhibited worse condition with faster respiratory rate and more weight loss compared to that in the A549-V group (Fig. S4C). The reversed effects were observed in H358-shV and H358-shZIP4 mice. H358-shZIP4 mice have less weight loss compared with control group (Fig. S4D). Three weeks after tumor implantation, mice were euthanized, and the pulmonary metastatic nodules were counted under the GFP filter. The number of metastatic nodules in the lung were significantly higher in A549-ZIP4 group than that in the A549-V mice (Fig. 3A and C). In contrast, H358-shZIP4 group mice showed reduced number of lung metastatic nodules than H358-shV group mice (Fig. 3B and D). The H&E staining results showed lung metastasis in all the mice. Therefore, these *in vivo* results further demonstrated that ZIP4 played an important role in NSCLC metastasis which is consistent with the *in vitro* data. In the subcutaneous mouse model, there were no significant difference of tumor weight in A549-V and A549-ZIP4, H358-shV and H358-shZIP4 groups (Fig. S3C - S3D, S3F - S3G). However, we found that the tumors in A549-ZIP4 mice group were prone to develop ulcer compared with A549-V group (Fig. S3E). These results further indicated that the effect we see in Fig. 3 is due to migration and invasion, but not proliferation.

3.4. ZIP4 is correlated with EMT markers in NSCLC cells and the mouse lung metastatic tumors

To gain further insight into possible downstream signaling pathways

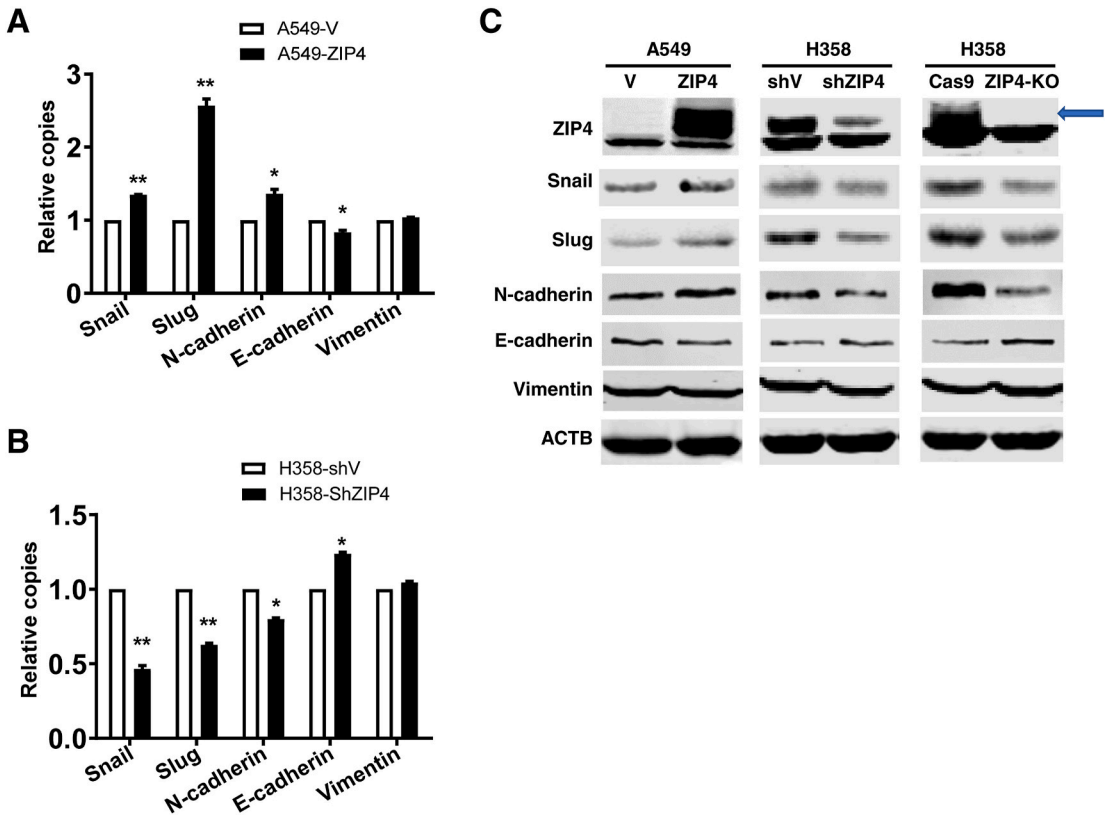

Fig. 4. ZIP4 regulates the expression of EMT markers in NSCLC cell lines. **(A)** Fold changes in mRNA levels of EMT markers Snail, Slug, N-cadherin, E-cadherin and Vimentin in A549-V and A549-ZIP4 cells shown by RT-PCR analysis. **(B)** Fold changes in mRNA levels of EMT markers Snail, Slug, N-cadherin, E-cadherin and Vimentin in H358-shV and H358-shZIP4 cells shown by RT-PCR analysis. **(C)** Protein levels of ZIP4 and EMT markers Snail, Slug, N-cadherin, E-cadherin and Vimentin in A549-V, A549-ZIP4, H358-shV, H358-shZIP4, H358-Cas9, H358-ZIP4-KO cells were detected by Western blot. ACTB was used as a loading control (Blue arrow indicates the ZIP4 band). All the results were repeated at least three times, and the average values were presented. $^{*}P < 0.05$; $^{**}P < 0.01$.

underlying the regulation of ZIP4 during NSCLC progression and metastasis, we performed the mechanistic study using both *in vitro* and *in vivo* assays. Since ZIP4 is correlated with EMT gene signatures in GSE30219 and GSE10072 datasets (Figs. S1D–S1E), we validated the gene expression correlations in the NSCLC cell lines with ZIP4 overexpression, knockdown and knockout. As shown in Fig. 4A and C and Fig. S5A, the expression of Snail, Slug and N-cadherin in A549- ZIP4 cells was upregulated at both mRNA and protein levels compared to A549-V cells. In contrast, H358 cells showed decreased Snail, Slug and N-cadherin expression following ZIP4 knockdown or knockout (Fig. 4B–C, Figs. S5B–S5C). The IHC staining results showed increased expression of Snail, Slug and N-cadherin in the xenograft mice lung metastatic tumors of A549-ZIP4 group comparing with A549-V group (Fig. 5AandB). ZIP4 expression was positively correlated with Snail ($P < 0.0001$, $r = 0.8077$), Slug ($P < 0.0001$, $r = 0.5622$) and N-cadherin ($P = 0.0067$, $r = 0.3278$) in the mice lung metastatic tumor tissues (Fig. 5C). Conversely, expression of Snail, Slug and N-cadherin in the mice lung metastatic tumors was decreased in H358-shZIP4 group compared with H358-shV (Fig. 5D and 5E) and ZIP4 expression was positively correlated with Snail ($P = 0.0021$, $r = 0.7144$), Slug ($P = 0.0392$, $r = 0.4311$) and N-cadherin ($P = 0.0038$, $r = 0.6695$) (Fig. 5F).

3.5. ZIP4 promotes NSCLC cells migration and invasion in a snail-dependent manner

Next, we further examined the mechanism that how ZIP4 enhances tumor metastasis through regulating these EMT gene expression. Snail is a crucial transcription factor that provokes EMT through converting epithelial cells into mesenchymal cells with migratory properties [20–22]. Our data showed that Snail is positively correlated with ZIP4 expression. Therefore, we hypothesized that Snail is involved in the process of tumor migration and invasion mediated by ZIP4. We performed the wound healing assay, transwell migration and invasion assay in A549-V and A549-ZIP4 cells with or without Snail silencing using RNAi technique. First, we used three siRNAs for Snail knockdown in A549-ZIP4 cells and the RNA interference efficiency was confirmed by RT-PCR and Western blot (Fig. 6A and 6B). The wound healing assay showed that A549-ZIP4 cells had significantly faster closure of the wound area than A549-V cells, but with Snail knockdown, the migration distance decreased in the A549-ZIP4 cells at 48 h (Fig. 6C). And the transwell assay results also showed that tumor migration and invasion induced by ZIP4 was impaired by Snail knockdown (Fig. 6D). The expression of N-cadherin decreased when knocking down Snail in A549-ZIP4 cells which indicates N-cadherin may act as the downstream of Snail in promoting NSCLC metastasis (Fig. 6E). As a result, Snail pathway may partially mediate ZIP4-induced migration and invasion in NSCLC cells (Fig. 7).

4. Discussion

Recent studies have indicated that ZIP4 plays important roles in tumor progression in many cancer types. However, its role in NSCLC pathogenesis and the underlying molecular mechanism remains unknown. In this study, we elucidated that ZIP4 was overexpressed in NSCLC and negatively correlated with patients' OS and PFS. ZIP4 promoted migration, invasion and metastasis of NSCLC *in vitro* and *in vivo*. We also demonstrated that Snail, a key transcriptional factor, is a mediator of ZIP4 pathway. And N-cadherin is the downstream of Snail involved in the process of NSCLC progression. These results help us to further understand the molecular functions of ZIP4 in NSCLC

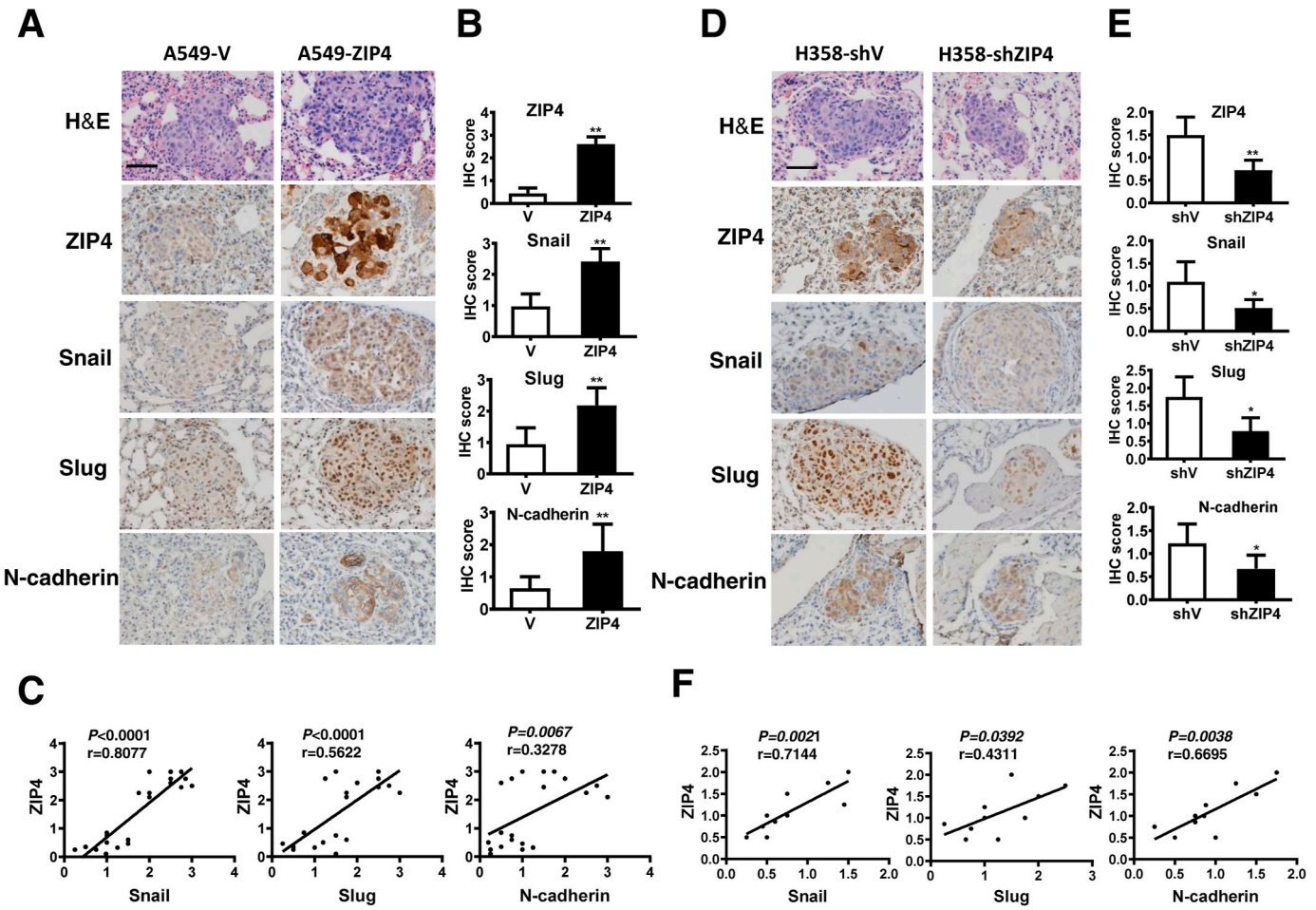

Fig. 5. ZIP4 is correlated with EMT markers in mice lung metastatic tumors. **(A)** Representative picture of H&E and IHC staining of ZIP4, Snail, Slug and N-cadherin in A549-V and A549-ZIP4 xenograft mice lung metastatic tumor tissues. **(B)** IHC score of ZIP4, Snail, Slug and N-cadherin staining in A549-V and A549-ZIP4 groups. **(C)** Correlations of ZIP4 with Snail ($P < 0.0001$, r = 0.8077), Slug ($P < 0.0001$, r = 0.5622) and N-cadherin ($P = 0.0067$, r = 0.3278) in A549-V and A549-ZIP4 xenograft mice lung metastatic tumor tissues. **(D)** Representative picture of H&E and IHC staining of ZIP4, Snail, Slug and N-cadherin in H358-shV and H358-shZIP4 xenograft mice lung metastatic tumor tissues. **(E)** IHC score of ZIP4, Snail, Slug and N-cadherin staining in H358-shV and H358-shZIP4 xenograft mouse groups. **(F)** Correlations of ZIP4 with Snail ($P = 0.0021$, r = 0.7144), Slug ($P = 0.0392$, r = 0.4311) and N-cadherin ($P = 0.0038$, r = 0.6695) in H358-shV and H358-shZIP4 xenograft mice lung metastatic tumor tissues. Pearson correlation coefficient was used to quantify the correlation between the expression of ZIP4 and EMT markers. $^{*}P < 0.05$; $^{**}P < 0.01$.

pathogenesis and inhibition of ZIP4 might be a novel treatment strategy for ZIP4-overexpressed NSCLC.

Previous studies have shown that zinc plays important roles in tumor progression and intracellular zinc level should be maintained at a fine balance by zinc transporters [7]. Zinc plays pivotal role in structural, catalytic, and normal regulatory functions, making it essential for the physiologic functioning of the human body [23]. Zinc deficiency was reported to be associated with different solid malignancies, including NSCLC [23,24]. Meanwhile, zinc is also involved in the immune response and anti-tumor effect, which suggested the importance of zinc homeostasis in cancer carcinogenesis and development [23,25]. As an essential zinc transporter, the impact of ZIP4 has been clearly established in pancreatic cancer (PC) [6,9,15,26], nasopharyngeal carcinoma (NPC) [27] and glioblastoma (GBM) [12] progression. Our group firstly identified that ZIP4 was overexpressed both in pancreatic cancer cell lines and surgical specimens of patients with PC [9]. Molecular mechanism studies found that ZIP4 can promote tumor growth, metastasis and chemoresistance in PC via a complex regulation network, which includes CREB-miR-373 axis [6], IL-6/STAT3 pathway [28] and ZEB1 dependent transcriptional mechanisms [26,29]. Overexpression of ZIP4 was also observed in ovarian cancer as an important cancer stem cell regulator [30,31]. Zeng et al. reported that ZIP4 expression level was associated with higher TNM staging and poor prognosis in patients with NPC, inhibition of ZIP4 reversed the EMT and enhanced radiosensitivity via the PI3K/Akt signaling pathway in NPC [27]. In NSCLC, our previous study identified that ZIP4 was overexpressed in six lung cancer cell lines [16]. However, the expression profile in lung cancer tissues and the exact molecular mechanisms have not been well explored. In this study, the expression analysis data from NSCLC TMA showed that ZIP4 expression was higher in NSCLC tissues than adjacent benign tissues and was negatively associated with patients' OS and PFS. Overexpression of ZIP4 promoted tumor migration and invasion *in vitro* while silencing of ZIP4 inhibited these processes. Our *in vivo* data showed that the number of lung metastatic nodules was significantly higher in ZIP4 overexpression mice and in contrast it was reduced in ZIP4 knockdown group. The *in vivo* xenograft model of lung cancer metastasis was established by injecting tumor cells via tail vein. Other than this tail vein model, current lung cancer metastasis mouse models also include intrathoracic implantation via puncture [32], or introducing the tumor cells into the trachea to the bronchus [33]. But due to the risk of pneumothorax, intrathoracic hemorrhage, hemoptysis and death in those models, the tail vein model has a unique advantage and has been used in several previous studies [18,19,34]. We recognize the limitation of the tail vein model as well, which does not fully recapitulate the

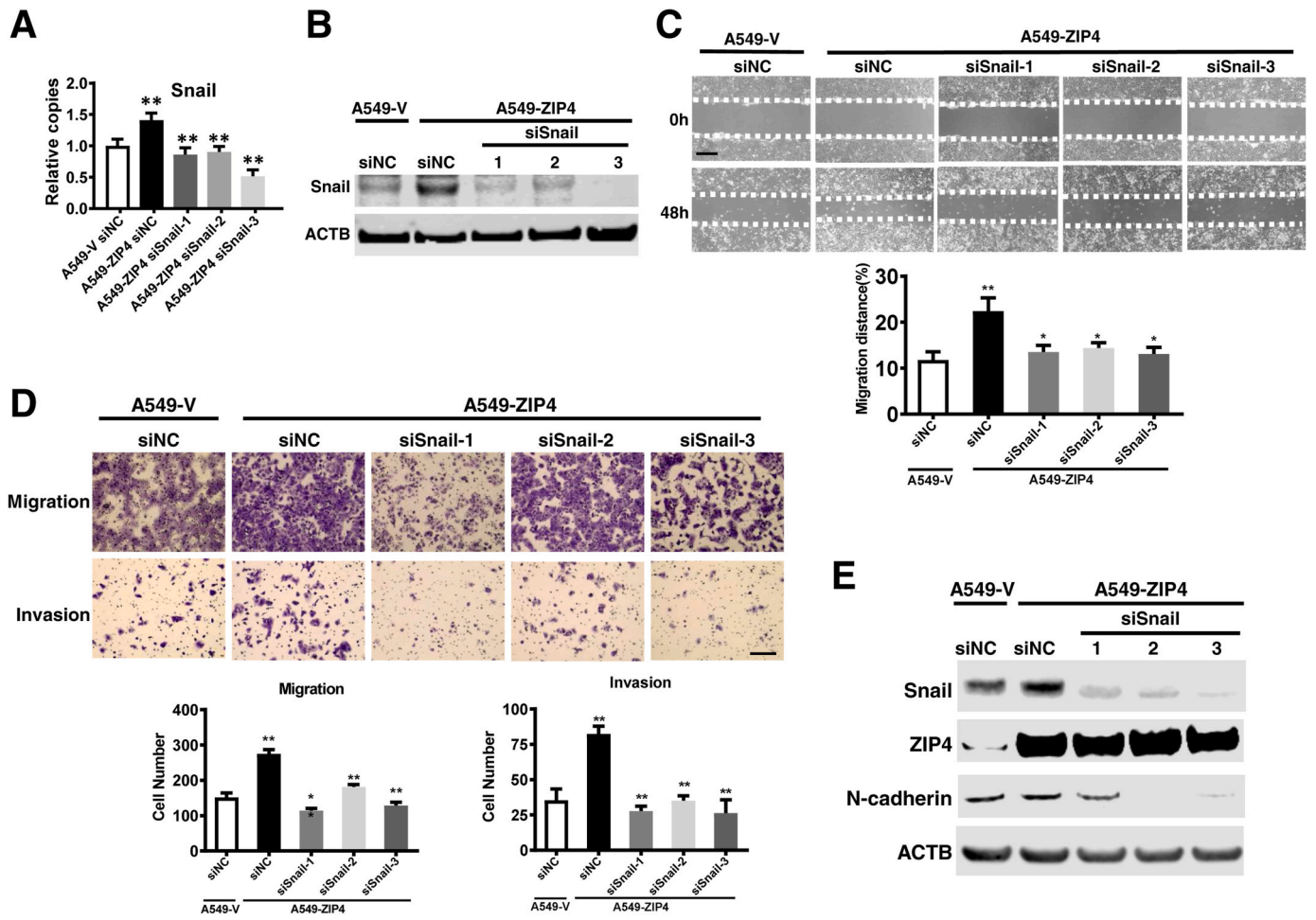

Fig. 6. ZIP4 promotes migration and invasion in a Snail-dependent manner in NSCLC cells. **(A)** siRNA knockdown efficiency of Snail in A549-V and A549-ZIP4 cells. Three siRNAs were used to transfected in A549-ZIP4 cells and siNC was the control siRNA. mRNA level of Snail detected by RT-PCR in A549-V siNC, A549-ZIP4 siNC, A549-ZIP4 siSnail-1, A549-ZIP4 siSnail-2, A549-ZIP4 siSnail-3. **(B)** Protein level of Snail detected by Western blot in A549-V siNC, A549-ZIP4 siNC, A549-ZIP4 siSnail-1, A549-ZIP4 siSnail-2, A549-ZIP4 siSnail-3. **(C)** Wound healing assay. The view of wound healing was captured at 0 and 48 h in A549-V siNC, A549-ZIP4 siNC and A549-ZIP4 siSnail-1, A549-ZIP4 siSnail-2, A549-ZIP4 siSnail-3. ($P < 0.01$, *t*-test, n = 10). Scale bar, 100 μm. **(D)** Transwell migration and invasion assay. Relative cell migration and invasion was detected in A549-V siNC, A549-ZIP4 siNC and A549-ZIP4 siSnail-1, A549-ZIP4 siSnail-2, A549-ZIP4 siSnail-3. ($P < 0.01$, *t*-test, n = 10). Scale bar, 100 μm. **(E)** Protein levels of Snail, ZIP4 and N-cadherin in A549-V siNC, A549-ZIP4 siNC and A549-ZIP4 siSnail-1, A549-ZIP4 siSnail-2, A549-ZIP4 siSnail-3 were detected by Western blot.

metastasis process of human lung cancer, more xenograft models or spontaneous lung cancer metastasis mouse models are warranted in future studies.

The degree of malignant NSCLC is high and most of the patients had metastasis at the time of diagnosis. Cell migration and invasion play critical roles in the process of tumor metastasis. A large number of previous studies have confirmed that EMT is activated in many malignant tumor cells, resulting in loss of typical epithelial cell characteristics and meanwhile gaining mesenchymal cell features to promote cancer cells dislocation, migration and complete the invasion-metastasis cascade [35,36]. Recent studies also revealed that EMT is a dynamic process with an intermediate status instead of binary phenotype. In this study, the database analysis from GSE30219 also revealed that ZIP4 was correlated with the cell component, molecular function, and biological developments. Of note, the bioinformatic analysis found that ZIP4 was associated with key regulatory genes in cancer cell EMT. A recent study from our group confirmed that ZIP4 activated ZEB1 and YAP1 to promote EMT plasticity and metastasis in pancreatic cancer [26]. These results suggested a pivotal role of ZIP4 in EMT plasticity in NSCLC. However, the exact molecular mechanisms remain to be elucidated. EMT transcriptional factors (EMT-TFs), including ZEB1, Snail and Twist etc., play a key role in EMT plasticity regulation. Snail was firstly reported to be involved in the formation of mesoderm in *Drosophila melanogaster* [37]. Three Snail family proteins were identified in human, including Snail 1 (Snail), Snail2 (Slug) and Snail 3 (Smuc) [38]. All Snail family members share a highly conserved C-terminal domain, this terminal domain contains 4–6 zinc fingers and can bind to the E-box motif in target gene promoters [39]. Snail has been confirmed to be regulated by various signal factors from the tumor microenvironment [38]. As a key regulator of EMT and cancer metastasis, the role of Snail in NSCLC development and progression has been studied in recent years. Yanagawa et al. reported that Snail was overexpressed in NSCLC tissue, and high expression of Snail was correlated with poor prognosis [40]. It can promote cancer angiogenesis and metastasis by CXCR2 ligands [40]. Li et al. found that SIRT6 deacetylates Snail and prevents its proteasomal degradation to promote EMT and metastasis in NSCLC [41]. Knockdown of Snail can also induce G2/M arrest and reverse EMT in NSCLC [42]. Deng et al. reported that G-protein-signaling modulator 2 (GPSM2) was downregulated in NSCLC tissues, the *in vitro* and *in vivo* studies revealed that knockdown of GPSM2 accelerated the EMT process through the ERK/GSK-3β/Snail pathway [43]. Snail also regulated the expression of Nanog, an important stem cell-like properties regulator, to mediate EMT plasticity in NSCLC [44]. In our study, we revealed that ZIP4 expression was correlated with the EMT marker genes expression, such as Snail,

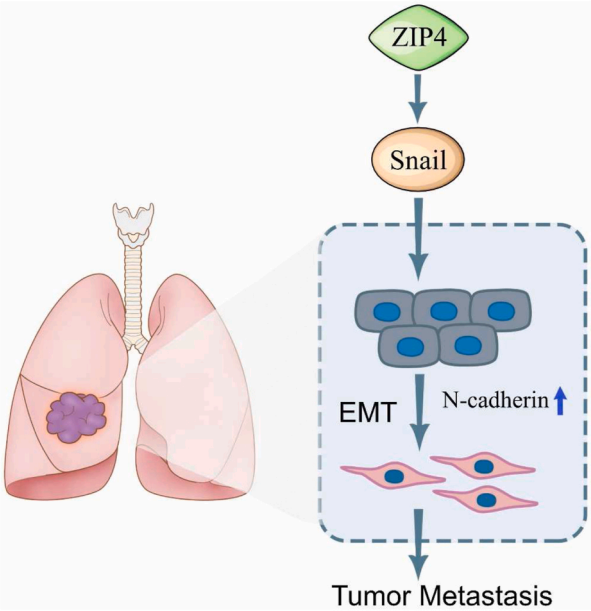

Fig. 7. Schematic diagram of ZIP4-Snail-EMT signaling pathway in NSCLC cells.
ZIP4 induced Snail expression and activity, and further activated N -cadherin to promote EMT and metastasis in NSCLC. A zinc dependent transcription factor Snail is a mediator of ZIP4 initiated signaling cascade, and N -cadherin is the downstream effector of Snail involved in the process of NSCLC progression and metastasis.

Slug and N-cadherin in NSCLC. Knockdown of ZIP4 prevented the metastasis in xenograft mouse model, and also inhibited the expression of Snail, Slug and N-cadherin. In contrast, overexpression of ZIP4 upregulates the expression of Snail, Slug and N-cadherin to promote metastasis in NSCLC. We also found that knockdown of Snail reversed the EMT process and inhibited the migration and invasion in ZIP4 overexpressed lung cancer cells. And the expression of N-cadherin was also reduced along with the Snail knockdown. These results confirmed that ZIP4 can promote EMT and metastasis in NSCLC by activating Snail-N-cadherin pathway. Since Snail is a zinc finger protein and homeodomain transcriptional factor, it may interact with ZIP4 directly to facilitate tumor progression and metastasis. However, the detailed underlying molecular mechanisms of how ZIP4 regulates Snail warrants further investigation in future study.

In conclusion, our study deciphered a novel pathway that ZIP4 induced Snail and further activated N-cadherin to promote tumor migration, invasion and metastasis in NSCLC. Our findings highlighted the potential value of ZIP4 as a useful prognostic biomarker and therapeutic target for NSCLC in the future.

Declaration of competing interest

The authors declare that they have no known competing financial interests or personal relationships that could have appeared to influence the work reported in this paper.

Acknowledgment

This work was partially supported by the Department of Medicine at OUHSC. We thank the Stephenson Cancer Center at OUHSC for the use of the Biostatistics Core and Small Animal Bioluminescent Imaging Core facilities.

Appendix A. Supplementary data

Supplementary data to this article can be found online at https://doi.org/10.1016/j.canlet.2021.08.025.

Author contributions

Study concept and design: Yuanyuan Jiang, Yuqing Zhang, Jingxuan Yang, Min Li. Acquisition of data: Yuanyuan Jiang, Hanxiang Zhan, Yuqing Zhang, Jingxuan Yang. Analysis and interpretation of data: Yuanyuan Jiang, Hanxiang Zhan, Yuqing Zhang, Jingxuan Yang, Mingyang Liu, Chao Xu, Junxia Zhang, Zhijun Zhou, Xiuhui Shi, Rajagopal Ramesh, Min Li. Writing and revision of the manuscript: Yuanyuan Jiang, Hanxiang Zhan, Yuqing Zhang, Jingxuan Yang, Mingyang Liu, Chao Xu, Xiao Fan, Junxia Zhang, Zhijun Zhou, Xiuhui Shi, Rajagopal Ramesh, and Min Li. All the authors have approved the final version of the paper.

References

[1] F. Bray, J. Ferlay, I. Soerjomataram, R.L. Siegel, L.A. Torre, A. Jemal, Global cancer statistics 2018: GLOBOCAN estimates of incidence and mortality worldwide for 36 cancers in 185 countries, CA Cancer J Clin 68 (2018) 394–424.
[2] R.L. Siegel, K.D. Miller, A. Jemal, Cancer statistics, CA Cancer J Clin 68 (2018) 7–30, 2018.
[3] Z. Chen, C.M. Fillmore, P.S. Hammerman, C.F. Kim, K.K. Wong, Non-small-cell lung cancers: a heterogeneous set of diseases, Nat. Rev. Canc. 14 (2014) 535–546.
[4] R.S. Herbst, D. Morgensztern, C. Boshoff, The biology and management of non-small cell lung cancer, Nature 553 (2018) 446–454.
[5] S.E. Rebuzzi, L. Zullo, G. Rossi, M. Grassi, V. Murianni, M. Tagliamento, A. Prelaj, S. Coco, L. Longo, M.G. Dal Bello, A. Alama, C. Dellepiane, E. Bennicelli, U. Malapelle, C. Genova, Novel emerging molecular targets in non-small cell lung cancer, Int. J. Mol. Sci. 22 (2021).
[6] Y. Zhang, J. Yang, X. Cui, Y. Chen, V.F. Zhu, J.P. Hagan, H. Wang, X. Yu, S. E. Hodges, J. Fang, P.J. Chiao, C.D. Logsdon, W.E. Fisher, F.C. Brunicardi, C. Chen, Q. Yao, M.E. Fernandez-Zapico, M. Li, A novel epigenetic CREB-miR-373 axis mediates ZIP4-induced pancreatic cancer growth, EMBO Mol. Med. 5 (2013) 1322–1334.
[7] T. Hara, T.A. Takeda, T. Takagishi, K. Fukue, T. Kambe, T. Fukada, Physiological roles of zinc transporters: molecular and genetic importance in zinc homeostasis, J. Physiol. Sci. 67 (2017) 283–301.
[8] T. Kambe, T. Tsuji, A. Hashimoto, N. Itsumura, The physiological, biochemical, and molecular roles of zinc transporters in zinc homeostasis and metabolism, Physiol. Rev. 95 (2015) 749–784.
[9] M. Li, Y. Zhang, Z. Liu, U. Bharadwaj, H. Wang, X. Wang, S. Zhang, J.P. Liuzzi, S. M. Chang, R.J. Cousins, W.E. Fisher, F.C. Brunicardi, C.D. Logsdon, C. Chen, Q. Yao, Aberrant expression of zinc transporter ZIP4 (SLC39A4) significantly contributes to human pancreatic cancer pathogenesis and progression, Proc. Natl. Acad. Sci. U. S. A. 104 (2007) 18636–18641.
[10] J. Yang, Y. Zhang, X. Cui, W. Yao, X. Yu, P. Cen, S.E. Hodges, W.E. Fisher, F. C. Brunicardi, C. Chen, Q. Yao, M. Li, Gene profile identifies zinc transporters differentially expressed in normal human organs and human pancreatic cancer, Curr. Mol. Med. 13 (2013) 401–409.
[11] X. Kang, R. Chen, J. Zhang, G. Li, P.G. Dai, C. Chen, H.J. Wang, Expression profile Analysis of zinc transporters (ZIP4, ZIP9, ZIP11, ZnT9) in gliomas and their correlation with IDH1 mutation status, Asian Pac. J. Cancer Prev. APJCP 16 (2015) 3355–3360.
[12] Y. Lin, Y. Chen, Y. Wang, J. Yang, V.F. Zhu, Y. Liu, X. Cui, L. Chen, W. Yan, T. Jiang, G.W. Hergenroeder, S.A. Fletcher, J.M. Levine, D.H. Kim, N. Tandon, J. J. Zhu, M. Li, ZIP4 is a novel molecular marker for glioma, Neuro Oncol. 15 (2013) 1008–1016.
[13] T. Takatani-Nakase, Zinc transporters and the progression of breast cancers, Biol. Pharm. Bull. 41 (2018) 1517–1522.
[14] R.B. Franklin, P. Feng, B. Milon, M.M. Desouki, K.K. Singh, A. Kajdacsy-Balla, O. Bagasra, L.C. Costello, hZIP1 zinc uptake transporter down regulation and zinc depletion in prostate cancer, Mol. Canc. 4 (2005) 32.
[15] M. Liu, Y. Zhang, J. Yang, X. Cui, Z. Zhou, H. Zhan, K. Ding, X. Tian, Z. Yang, K. A. Fung, B.H. Edil, R.G. Postier, M.S. Bronze, M.E. Fernandez-Zapico, M. P. Stemmler, T. Brabletz, Y.P. Li, C.W. Houchen, M. Li, ZIP4 increases expression of transcription factor ZEB1 to promote integrin alpha3beta1 signaling and inhibit expression of the gemcitabine transporter ENT1 in pancreatic cancer cells, Gastroenterology 158 (2020) 679–692, e671.
[16] C. Huang, X. Cui, X. Sun, J. Yang, M. Li, Zinc transporters are differentially expressed in human non-small cell lung cancer, Oncotarget 7 (2016) 66935–66943.
[17] C. Dong, B. Zhao, F. Long, Y. Liu, Z. Liu, S. Li, X. Yang, D. Sun, H. Wang, Q. Liu, R. Liang, Y. Li, Z. Gao, S. Shao, Q.R. Miao, L. Wang, Nogo-B receptor promotes the chemoresistance of human hepatocellular carcinoma via the ubiquitination of p53 protein, Oncotarget 7 (2016) 8850–8865.
[18] U. Jarry, M. Bostoen, R. Pineau, L. Chaillot, V. Mennessier, P. Montagne, E. Motte, M. Gournay, A. Le Goff, T. Guillaudeux, R. Pedeux, Orthotopic model of lung

cancer: isolation of bone micro-metastases after tumor escape from Osimertinib treatment, BMC Canc. 21 (2021) 530.
[19] N. Shrestha, Z. Lateef, O. Martey, A.R. Bland, M. Nimick, R. Rosengren, J. C. Ashton, Does the mouse tail vein injection method provide a good model of lung cancer? F1000Res 8 (2019) 190.
[20] J. Gao, L. Tian, Y. Sun, W. Li, L. Zhao, Y. Sun, Z. Jing, L. Zhou, F. Liu, X. Zhao, PURalpha mediates epithelial-mesenchymal transition to promote esophageal squamous cell carcinoma progression by regulating Snail2, Canc. Lett. 498 (2021) 98–110.
[21] L. Li, H. Zhou, R. Zhu, Z. Liu, USP26 promotes esophageal squamous cell carcinoma metastasis through stabilizing Snail, Canc. Lett. 448 (2019) 52–60.
[22] I. Georgakopoulos-Soares, D.V. Chartoumpekis, V. Kyriazopoulou, A. Zaravinos, EMT factors and metabolic pathways in cancer, Front Oncol 10 (2020) 499.
[23] D. Skrajnowska, B. Bobrowska-Korczak, Role of zinc in immune system and anti-cancer defense mechanisms, Nutrients 11 (2019).
[24] Y. Wang, Z. Sun, A. Li, Y. Zhang, Association between serum zinc levels and lung cancer: a meta-analysis of observational studies, World J. Surg. Oncol. 17 (2019) 78.
[25] S. Hojyo, T. Fukada, Roles of zinc signaling in the immune system, J Immunol Res 2016 (2016) 6762343.
[26] M. Liu, Y. Zhang, J. Yang, H. Zhan, Z. Zhou, Y. Jiang, X. Shi, X. Fan, J. Zhang, W. Luo, K.A. Fung, C. Xu, M.S. Bronze, C.W. Houchen, M. Li, Zinc-dependent regulation of ZEB1 and YAP1 coactivation promotes epithelial-mesenchymal transition plasticity and metastasis in pancreatic cancer, Gastroenterology 160 (2021) 1771–1783, e1771.
[27] Q. Zeng, Y.M. Liu, J. Liu, J. Han, J.X. Guo, S. Lu, X.M. Huang, P. Yi, J.Y. Lang, P. Zhang, C.T. Wang, Inhibition of ZIP4 reverses epithelial-to-mesenchymal transition and enhances the radiosensitivity in human nasopharyngeal carcinoma cells, Cell Death Dis. 10 (2019) 588.
[28] Y. Zhang, U. Bharadwaj, C.D. Logsdon, C. Chen, Q. Yao, M. Li, ZIP4 regulates pancreatic cancer cell growth by activating IL-6/STAT3 pathway through zinc finger transcription factor CREB, Clin. Canc. Res. 16 (2010) 1423–1430.
[29] M. Liu, J. Yang, Y. Zhang, Z. Zhou, X. Cui, L. Zhang, K.M. Fung, W. Zheng, F. D. Allard, E.U. Yee, K. Ding, H. Wu, Z. Liang, L. Zheng, M.E. Fernandez-Zapico, Y. P. Li, M.S. Bronze, K.T. Morris, R.G. Postier, C.W. Houchen, J. Yang, M. Li, ZIP4 promotes pancreatic cancer progression by repressing ZO-1 and claudin-1 through a ZEB1-dependent transcriptional mechanism, Clin. Canc. Res. 24 (2018) 3186–3196.
[30] Q. Fan, Q. Cai, P. Li, W. Wang, J. Wang, E. Gerry, T.L. Wang, I.M. Shih, K. P. Nephew, Y. Xu, The novel ZIP4 regulation and its role in ovarian cancer, Oncotarget 8 (2017) 90090–90107.
[31] Q. Fan, W. Zhang, R.E. Emerson, Y. Xu, ZIP4 is a novel cancer stem cell marker in high-grade serous ovarian cancer, Cancers (2020) 12.
[32] X. Liu, J. Liu, Y. Guan, H. Li, L. Huang, H. Tang, J. He, Establishment of an orthotopic lung cancer model in nude mice and its evaluation by spiral CT, J. Thorac. Dis. 4 (2012) 141–145.
[33] T. Nakajima, T. Anayama, Y. Matsuda, D.M. Hwang, P.Z. McVeigh, B.C. Wilson, G. Zheng, S. Keshavjee, K. Yasufuku, Orthotopic lung cancer murine model by nonoperative transbronchial approach, Ann. Thorac. Surg. 97 (2014) 1771–1775.
[34] M. Zhao, A. Suetsugu, H. Ma, L. Zhang, F. Liu, Y. Zhang, B. Tran, R.M. Hoffman, Efficacy against lung metastasis with a tumor-targeting mutant of Salmonella typhimurium in immunocompetent mice, Cell Cycle 11 (2012) 187–193.
[35] Y. Jiang, H. Zhan, Communication between EMT and PD-L1 signaling: new insights into tumor immune evasion, Canc. Lett. 468 (2020) 72–81.
[36] T. Brabletz, R. Kalluri, M.A. Nieto, R.A. Weinberg, EMT in cancer, Nat. Rev. Canc. 18 (2018) 128–134.
[37] A. Alberga, J.L. Boulay, E. Kempe, C. Dennefeld, M. Haenlin, The snail gene required for mesoderm formation in Drosophila is expressed dynamically in derivatives of all three germ layers, Development 111 (1991) 983–992.
[38] Y. Wang, J. Shi, K. Chai, X. Ying, B.P. Zhou, The role of snail in EMT and tumorigenesis, Curr. Cancer Drug Targets 13 (2013) 963–972.
[39] M.A. Nieto, The snail superfamily of zinc-finger transcription factors, Nat. Rev. Mol. Cell Biol. 3 (2002) 155–166.
[40] J. Yanagawa, T.C. Walser, L.X. Zhu, L. Hong, M.C. Fishbein, V. Mah, D. Chia, L. Goodglick, D.A. Elashoff, J. Luo, C.E. Magyar, M. Dohadwala, J.M. Lee, M.A. St John, R.M. Strieter, S. Sharma, S.M. Dubinett, Snail promotes CXCR2 ligand-dependent tumor progression in non-small cell lung carcinoma, Clin. Canc. Res. 15 (2009) 6820–6829.
[41] Z. Li, J. Huang, S. Shen, Z. Ding, Q. Luo, Z. Chen, S. Lu, SIRT6 drives epithelial-to-mesenchymal transition and metastasis in non-small cell lung cancer via snail-dependent transrepression of KLF4, J. Exp. Clin. Canc. Res. 37 (2018) 323.
[42] X. Yang, M. Han, H. Han, B. Wang, S. Li, Z. Zhang, W. Zhao, Silencing Snail suppresses tumor cell proliferation and invasion by reversing epithelial-to-mesenchymal transition and arresting G2/M phase in non-small cell lung cancer, Int. J. Oncol. 50 (2017) 1251–1260.
[43] M. Deng, B. Liu, Z. Zhang, Y. Chen, Y. Wang, X. Wang, Q. Lv, X. Yang, K. Hou, X. Che, X. Qu, Y. Liu, Y. Zhang, X. Hu, Knockdown of G-protein-signaling modulator 2 promotes metastasis of non-small-cell lung cancer by inducing the expression of Snail, Canc. Sci. 111 (2020) 3210–3221.
[44] C.W. Liu, C.H. Li, Y.J. Peng, Y.W. Cheng, H.W. Chen, P.L. Liao, J.J. Kang, M. H. Yeng, Snail regulates Nanog status during the epithelial-mesenchymal transition via the Smad 1/Akt/GSK3beta signaling pathway in non-small-cell lung cancer, Oncotarget 5 (2014) 3880–3894.